

Relativistic calculations of fine-structure energy levels of He-like Ar in dense plasmas

Xiang-Fu Li(李向富), Gang Jiang(蒋刚)

Citation: Chin. Phys. B . 2018, 27(7): 073101. **doi:** 10.1088/1674-1056/27/7/073101

Journal homepage: http://cpb.iphy.ac.cn; http://iopscience.iop.org/cpb

What follows is a list of articles you may be interested in

---

tomic structure and transition properties of H-like Al in hot and dense plasmas

Xiang-Fu Li(李向富), Gang Jiang(蒋刚), Hong-Bin Wang(王宏斌), Qian Sun(孙乾)

Chin. Phys. B . 2017, 26(1): 013101. **doi:** 10.1088/1674-1056/26/1/013101

Calculations of the dynamic dipole polarizabilities for the Li^+ ion

Yong-Hui Zhang(张永慧), Li-Yan Tang(唐丽艳), Xian-Zhou Zhang(张现周), Ting-Yun Shi(史庭云)

Chin. Phys. B . 2016, 25(10): 103101. **doi:** 10.1088/1674-1056/25/10/103101

Tune-out wavelengths for the alkaline-metal atoms

Wei-Wei Yu(于伟威), Rong-Mei Yu(于荣梅), Yong-Jun Cheng(程勇军) and Ya-Jun Zhou(周雅君)

Chin. Phys. B . 2016, 25(2): 023101. **doi:** 10.1088/1674-1056/25/2/023101

High-precision spectroscopy of hydrogen molecular ions

Zhong Zhen-Xiang, Tong Xin, Yan Zong-Chao, Shi Ting-Yun

Chin. Phys. B . 2015, 24(5): 053102. **doi:** 10.1088/1674-1056/24/5/053102

Precision calculation of fine structure in helium and Li^+

Zhang Pei-Pei, Zhong Zhen-Xiang, Yan Zong-Chao, Shi Ting-Yun

Chin. Phys. B . 2015, 24(3): 033101. **doi:** 10.1088/1674-1056/24/3/033101

Relativistic calculations of fine-structure energy levels of He-like Ar in dense plasmas*

Xiang-Fu Li(李向富)[1,2] and Gang Jiang(蒋刚)[1,3,†]

[1] Institute of Atomic and Molecular Physics, Sichuan University, Chengdu 610065, China
[2] College of Electrical Engineering, Longdong University, Qingyang 745000, China
[3] Key Laboratory of High Energy Density Physics and Technology, Ministry of Education, Chengdu 610065, China

(Received 26 May 2018; published online 25 June 2018)

The fine-structure energy levels of 1s2s and 1s2p atomic states for the He-like Ar ion immersed in dense plasmas are calculated. The ion sphere model is used to describe the plasma screening effect on the tested ion. The influences of the hard sphere confinement and plasma screening on the fine-structure energy levels are investigated respectively. The calculated results show that the confined effect of the hard sphere on the fine-structure energy levels increases with decreasing hard sphere radius, and the plasma screening effect on the fine-structure energy levels increases with the increase of free electron density. In dense plasmas, the confined effect of the hard sphere on the fine-structure energy levels can be neglected generally, compared with the contribution from free electron screening. An interesting phenomenon about the energy level crossing is found among 1s2s ($^1S_0$) and 1s2p ($^3P_{0,1}$) atomic states. The results reported at the present work are useful for plasma diagnostics.

Keywords: He-like Ar, fine-structure energy levels, hard sphere confinement, free electron screening

PACS: 31.15.ac, 31.15.ag, 31.15.xr, 52.27.Gr **DOI:** 10.1088/1674-1056/27/7/073101

1. Introduction

The dense plasma state is a common phase of matter in the universe and can be found in all types of stars and within giant planets.[1] Dense plasmas are commonly created in experiments involving high-power light sources, such as the National Ignition Facility,[2] recently developed x-ray free-electron laser Linac Coherent Light Source (LCLS) (USA)[3] and SACLA (Japan).[4] In dense plasmas, the potential in and near an ion is influenced by its bound electrons, free electrons, and neighboring ions. Consequently, the phenomena, such as spectral line shifts, ionization potential depression (IPD), line merging, fine-structure energy level changes, energy level crossing, and continuum states lowering, could be observed. Such properties can effectively be utilized for inertial confinement fusion (ICF) plasma diagnostics and the investigation of x-ray opacity of matter under conditions prevailing in stellar interiors.

Several dense plasma experiments[5–9] about IPD have been performed recently by intense short-pulse laser irradiation. However, the widely used theoretical expression for the IPD given by Ecker and Kröll (EK)[10] or Stewart and Pyatt (SP)[11] cannot give a satisfied description for all of these experiments. The experimental results[5] about the critical electron densities of the He-like Al ion, after which spectral lines disappear, seem more consistent with SP model, but Ciricosta's experiments[6,7] about the direct measurements on the ionization energy of the K-shell in aluminum and the subsequent K_α lines tend to confirm EK model. It is inexplicable that the reported experimental results by Kraus *et al.*[9] could not be explained using either of the two theoretical models. One important reason for this circumstance is the lack of knowledge on the response of the fine-structure of the ions embedded in dense plasmas, e.g., the changes of the relative energy level order and the changes of transition probabilities. These effects play a crucial role for precise simulation of the final radiation from the plasma (spectral distribution) and for the precise diagnostic of plasma parameters.[12]

The fine-structure energy levels of 1s4l (l = s, p, d) atomic states for the He-like Al ions immersed in dense plasmas were calculated by Belkhiri *et al.*[13] using the ion sphere model (ISM).[14] The impact of dense plasma environments on the 1s3l (l = s, p, d) fine-structure levels of He-like ions (Z = 7–12) and thirty bound fine-structure levels of He-like Al ions were calculated by Li *et al.*[12,15] using the self-consistent-field ion sphere model (SCFISM).[16] De *et al.*[17] studied the effects of oscillatory quantum plasma screening on the fine-structure splitting between the components of Lyman-α and β line doublets of atomic hydrogen and hydrgen-like argon ion within dense quantum plasmas. To our knowledge, the fine-structure energy levels of the He-like Ar ion immersed in dense plasmas so far have not been reported. There are only several theoretical studies about the atomic structures of the He-like Ar ion within dense plasmas. The nonrelativistic en-

*Project supported by the National Natural Science Foundation of China (Grant No. 11474208) and the Doctoral Science Foundation of Longdong University, China (Grant No. XYBY1704).

†Corresponding author. E-mail: gjiang@scu.edu.cn

© 2018 Chinese Physical Society and IOP Publishing Ltd

ergy values of 1sns (^{1}S^e) (n = 1–3) and 1snp(^{1}P^o) (n = 2–4) states of the He-like Ar ion within dense plasma environment were estimated by Bhattacharyya *et al.*[18] based on the ISM. Sil *et al.*[19] used the ISM to estimate the effects of dense plasma on the He-like Ar ion within the non-relativistic as well as the relativistic framework, and the results showed that the relativistic scheme represented a relatively good agreement with the experiment.[20] The ionization potentials and excitation energies of the Ar^{16+} ion embedded in plasma environment were calculated by Das *et al.*[21] for the first time using the state-of-the-art coupled cluster-based linear response theory with the four-component relativistic spinors, and their results showed that the transition energies obtained from the relativistic calculations were in promising agreement with the experiment.[20]

In this work, the ISM is used to describe the plasma screening effect on the He-like Ar ion. It is electrical neutrality outside of the ion sphere, so the wavefunctions of bound electrons are not allowed to stretch outside of the ion sphere. That is, the ion sphere actually becomes an impenetrable cavity or hard sphere. Therefore, when the tested ion immersed in dense plasmas, it will experience not only the screening effect from free electrons, but also the confined effect from the hard sphere. We firstly calculate the fine-structure energy levels of the He-like Ar ion located in the hard sphere (not plasma environment), in order to estimate the confined effect of the hard sphere. We then calculate the fine-structure energy levels of the He-like Ar ion within dense plasmas, and discuss the influence of plasma environment on the fine-structure energy levels. Lastly, we compare the relative importance of the effects of hard sphere confinement and plasma screening on the fine-structure energy levels of the He-like Ar ion immersed in dense plasmas. The free electron density range chosen in this paper is from 2.06×10^{23} to 7.52×10^{25} cm^{-3}.

2. Theoretical method

The ISM is based on the principles that the ion is represented by a point-like nucleus with charge Z embedded at the centre of a spherical cavity containing enough electrons to ensure global neutrality. The spherical cavity is called as an ion sphere or Wigner–Seitz sphere. The ion sphere radius R_0 is determined by the formula $4\pi R_0^3 n_{\rm f}/3 = Z - N_{\rm b}$, where $n_{\rm f}$ is the free electron density and $N_{\rm b}$ is the number of bound electrons. The plasma is assumed to produce an electrically neutral background beyond the ion sphere radius R_0. For a N-electron atom, the Dirac–Coulomb Hamiltonian containing all of the dominant interactions can be written as

$$H = \sum_{i=1}^{N} H_i + \sum_{i=1}^{N-1}\sum_{j=i+1}^{N}\frac{1}{r_{ij}}, \tag{1}$$

where the first term is the contribution from one-body and the second term in the sum is the interaction between bound electrons. H_i is defined as

$$H_i = c\boldsymbol{\alpha}\cdot\boldsymbol{p}_i + (\beta-1)c^2 + V_{\rm IS}(r_i), \tag{2}$$

where the first and the second terms are the relativistic kinetic energy of a bound electron. The last term $V_{\rm IS}(r_i)$ is the modified potential as "seen" by one bound electron within the ion sphere, and is given by

$$V_{\rm IS}(r) = -\frac{Z}{r} + \frac{Z-N_{\rm b}}{2R_0}\left[3-\left(\frac{r}{R_0}\right)^2\right]. \tag{3}$$

The radial wavefunctions of bound electrons are derived by the Dirac equations[22]

$$\left(\frac{\mathrm{d}}{\mathrm{d}r}+\frac{k}{r}\right)P_{nk}(r) - \frac{1}{c}[2c^2-\varepsilon_{nk}+V_{\rm IS}(r)]Q_{nk}(r) = -X^P(r), \tag{4}$$

$$\left(\frac{\mathrm{d}}{\mathrm{d}r}-\frac{k}{r}\right)Q_{nk}(r) + \frac{1}{c}[-\varepsilon_{nk}+V_{\rm IS}(r)]P_{nk}(r) = X^Q(r), \tag{5}$$

where $P_{nk}(r)$ and $Q_{nk}(r)$ are the large and small components of the radial wavefunctions, respectively. Here ε_{nk} is the orbital energy eigenvalue and n is the principal quantum number. The spin-orbital quantum number $k=-l-1$ for $j=l+1/2$, or $k=l$ for $j=l-1/2$. $X^P(r)$ and $X^Q(r)$ are the exchange potentials which force the orthogonality between orbits of the same symmetry. With regard to the electrically neutral conditions supposed by the ISM, the radial wavefunctions $P_{nk}(r)$ and $Q_{nk}(r)$ are assumed to satisfy the boundary conditions and normalization condition respectively, namely,

$$X(0)=0, \quad X(r)=0, \quad X=P_{nk} \text{ or } Q_{nk}, \quad r\geq R_0, \tag{6}$$

$$\int_0^{R_0}[P_{nk}^2(r)+Q_{nk}^2(r)]\mathrm{d}r = 1. \tag{7}$$

Once the contributions of nuclear charge, bound electrons, and free electrons are included in the total Hamiltonian, the single-electron wavefunction can be obtained via the self-consistent-field method, which is carried out using the modified GRASP2K code.[23,24] By the way, the theory for the calculated atomic structures under the hard sphere confinement (not plasma environment) is very similar to that of the ISM mentioned above, except that the second term in Eq. (3) is equal to zero, namely, the free electron density is equal to zero. Thus the theoretical method for calculating atomic structures under the hard sphere confinement is not repeated here.

3. Results and discussion

3.1. Fine-structure energy levels of free He-like Ar

In this work, the multiconfiguration Dirac–Fock (MCDF) method is used to describe the correlation effect and relativistic effect. An atomic state function (ASF) is constructed approximately by a linear combination of configuration state functions (CSFs) with the same parity and angular momentum.

The CSFs are constructed by double exciting bound electrons in the occupied orbits of the reference CSFs to the unoccupied orbits. The configurations $1s^2$ and 1s2p are double excited to orbits nl ($n = 1, 2$, $l =$ s, p), in order to form the CSFs.

The energy eigenvalues and energy levels of $1s^2$, 1s2s, and 1s2p atomic states for the free He-like Ar ion are listed in Table 1. The table shows that our calculated energy levels of 1s2s and 1s2p atomic states agree well with those of NIST.[25] In addition, one point should be mentioned here that the correlation effect between bound electrons may not be considered very enough. The reasons are explained below. When the atomic structures of He-like Ar ions immersed in dense plasmas are calculated and the free electron densities are greater than 9.39×10^{24} cm^{-3} ($R_0 < 1.4$ a.u.), the bound electrons in the occupied orbits of the reference CSFs could not be excited to the higher unoccupied orbits, such as $3l$ ($l =$ s, p, and d) orbits, due to the confinement from the hard sphere. The CSFs for one ASF in both plasmas and vacuum should be the same as each other, or else the estimated intensity of plasma screening effect on the atomic structures is meaningless. Therefore, the only orbits nl ($n = 1, 2$, $l =$ s, p) are used to construct CSFs in both plasmas and vacuum, in order to describe the correlation effect between bound electrons.

Table 1. The energy eigenvalues E_b (in a.u.) and energy levels E_l (in cm^{-1}) of $1s^2$, 1s2s, and 1s2p atomic states for the free He-like Ar ion.

State	Term	J	E_b	E_l	E_l[25]	Dif%
$1s^2$	$^1S^e$	0	–314.1518215	0	0	0
1s2s	$^3S^e$	1	–200.0611286	25040012	25036648	0.013
	$^1S^e$	0	–199.3047447	25206019	25200962	0.020
1s2p	$^3P^o$	0	–199.3914879	25186981	25187806	0.003
	$^3P^o$	1	–199.3498879	25196111	25193007	0.012
	$^3P^o$	2	–199.2427388	25219628	25215229	0.017
	$^1P^o$	1	–198.7390167	25330182	25322441	0.031

3.2. Fine-structure energy levels under the hard sphere confinement (not plasma environment)

The energy eigenvalues of $1s^2$, 1s2s, and 1s2p atomic states for the He-like Ar ion under the hard sphere confinement are listed in Table 2. It can seen that all energy eigenvalues change very slightly with the hard sphere radius, and all of them shift to continuum state with decreasing hard sphere radius. The energy eigenvalues of all atomic states for the He-like Ar ion under the hard sphere confinement increase with the reduction of hard sphere radius, which is consistent with the reported results of the other confined two electron systems.[26–28] Figure 1 shows that the sequence of fine-structure energy levels of the He-like Ar ion under the hard sphere confinement is the same as that of the free case (see Table 1), but all energy levels move slightly. In order to more clearly display the energy level changes, the energy level shift is defined here, which is the difference between the energy level under hard sphere confinement and that in free case. The energy level shifts of 1s2s and 1s2p atomic states for the He-like Ar ion under the hard sphere confinement are displayed in Fig. 2. It can be seen that all energy levels shift upward. The smaller radius of the hard sphere is, the greater extent of the energy level shifts. The reason for this result showed from Table 2 and Fig. 3 is that the energy eigenvalue of $1s^2$ is nearly unchanged but those of 1s2s and 1s2p atomic states increase relatively greater with the decrease of hard sphere radius. In addition, the energy eigenvalues of $1s^2$ ($^1S_0$), 1s2s ($^1S_0$, $^3S_1$), and 1s2p ($^1P_1$, $^3P_{0,1,2}$) atomic states for the He-like Ar ion under hard sphere confinement are not reported for $R_0 \leq 0.7$ a.u., because the calculated data by our program become unstable for $R_0 \leq 0.7$ a.u., namely, the calculated data change with step size. The calculated data must be stable for different step size, otherwise the calculated data is unreliable.

Table 2. The energy eigenvalues E (in a.u.) of $1s^2$, 1s2s, and 1s2p atomic states for the He-like Ar ion under the hard sphere confinement.

R_0/a.u.	$1s^2$ ($^1S_0$)	1s2s ($^3S_1$)	1s2s ($^1S_0$)	1s2p ($^3P_0$)	1s2p ($^3P_1$)	1s2p ($^3P_2$)	1s2p ($^1P_1$)
∞	–314.1518215	–200.0611286	–199.3047447	–199.3914879	–199.3498879	–199.2427388	–198.7390167
1.8	–314.1518215	–200.0611286	–199.3047447	–199.3914879	–199.3498879	–199.2427388	–198.7390167
1.7	–314.1518215	–200.0611285	–199.3047446	–199.3914877	–199.3498878	–199.2427388	–198.7390167
1.6	–314.1518215	–200.0611279	–199.3047439	–199.3914873	–199.3498874	–199.2427384	–198.7390164
1.5	–314.1518215	–200.0611259	–199.3047417	–199.3914866	–199.3498866	–199.2427373	–198.7390152
1.4	–314.1518213	–200.0611192	–199.3047340	–199.3914835	–199.3498833	–199.2427336	–198.7390112
1.3	–314.1518209	–200.0610945	–199.3047057	–199.3914721	–199.3498714	–199.2427199	–198.7389967
1.2	–314.1518201	–200.0610096	–199.3046062	–199.3914337	–199.3498308	–199.2426726	–198.7389460
1.1	–314.1518192	–200.0607308	–199.3042702	–199.3913088	199.3496981	–199.2425146	–198.7387746
1.0	–314.1518179	–200.0598667	–199.3031905	–199.3909273	–199.3492874	–199.2420116	–198.7382207
0.9	–314.1518143	–200.0573415	–199.2998848	–199.3898485	–199.3481046	–199.2405000	–198.7365283
0.8	–314.1518094	–200.0509506	–199.2907877	–199.3871251	–199.3450226	–199.2362855	–198.7316666
0.7	–314.1518017	–200.0364787	–199.2675312	–199.3813327	–199.3380533	–199.2255825	–198.7188170

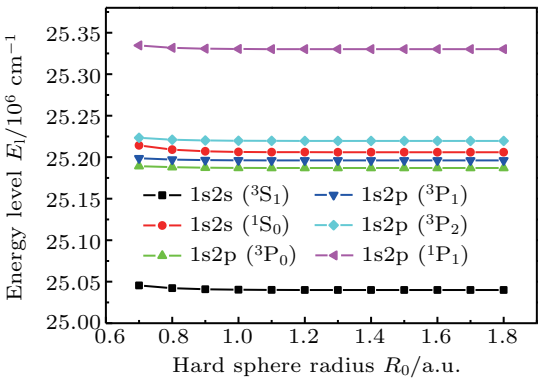


Fig. 1. (color online) The energy levels of 1s2s and 1s2p atomic states for the He-like Ar ion under the hard sphere confinement.

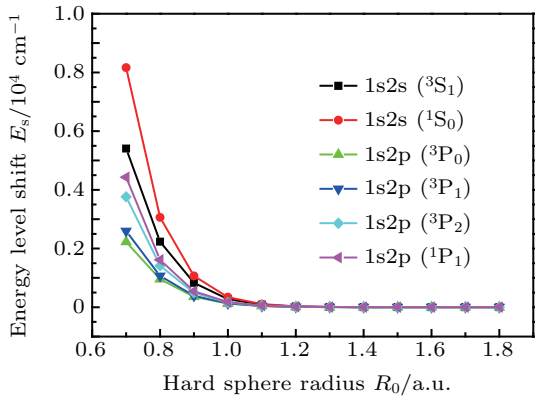


Fig. 2. (color online) The energy level shifts of 1s2s and 1s2p atomic states for the He-like Ar ion under the hard sphere confinement.

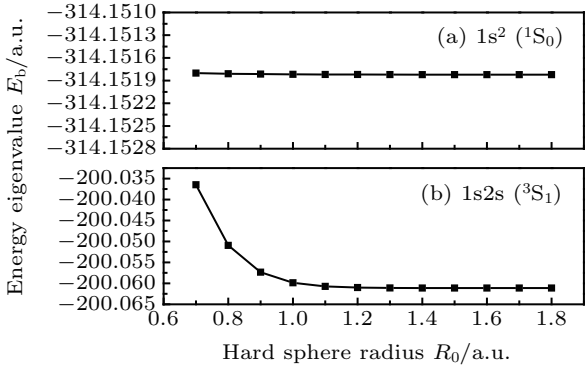


Fig. 3. The energy eigenvalues of 1s^2 (^{1}S$_0$) and 1s2s (^{3}S$_1$) atomic states for the He-like Ar ion under the hard sphere confinement. By the way, the variation trend of 1s2s (^{1}S$_0$) and 1s2p (^{3}P$_{0,1,2}$ and ^{1}P$_1$) atomic states with hard sphere radius is the same as that of 1s2s (^{3}S$_1$) atomic state.

It is also shown from Fig. 1 that the separation between the adjacent energy levels is slightly changed with the hard sphere radius. To more clearly investigate the variation of energy level separation with the hard sphere radius, the energy level separation shift is used here. The energy level separation shift is the difference between energy level separation under the hard sphere confinement and that in free case. As shown in Fig. 4, when the hard sphere radius is gradually decreased, the separations between 1s2s (^{3}S$_1$) and its lower adjacent level 1s^2 (^{1}S$_0$), 1s2s (^{1}S$_0$) and its lower adjacent level 1s2p (^{3}P$_1$) are remarkably increased, the energy level separations between 1s2p (^{3}P$_1$), 1s2p (^{1}P$_1$) and their adjacent lower atomic states are slightly increased respectively, but the energy level separations between 1s2p (^{3}P$_0$), 1s2p (^{3}P$_2$) and their adjacent lower atomic states are significant decreased respectively. In a word, the energy level separation shift under the hard sphere confinement is different for different energy levels.

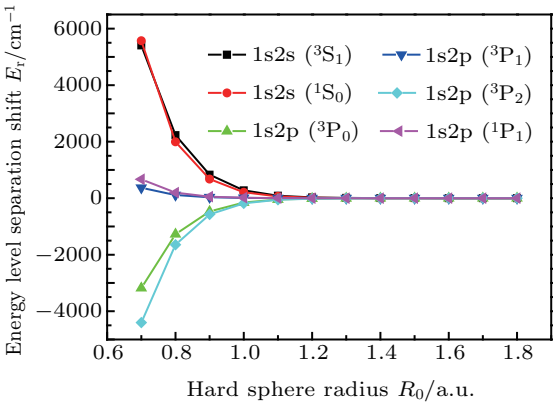


Fig. 4. (color online) The energy level separation shifts of 1s2s and 1s2p atomic states for the He-like Ar ion under the hard sphere confinement. 1s2s (^{3}S$_1$), 1s2s (^{1}S$_0$), 1s2p (^{3}P$_0$), 1s2p (^{3}P$_1$), 1s2p (^{3}P$_2$), and 1s2p (^{1}P$_1$) represent the energy level separations between 1s2s (^{3}S$_1$) and 1s^2 (^{1}S$_0$), 1s2s (^{1}S$_0$) and 1s2p (^{3}P$_1$), 1s2p (^{3}P$_0$) and 1s2s (^{3}S$_1$), 1s2p (^{3}P$_1$) and 1s2p (^{3}P$_0$), 1s2p (^{3}P$_2$) and 1s2s (^{1}S$_0$), and 1s2p (^{1}P$_1$) and 1s2p (^{3}P$_2$) atomic states, respectively.

It can be concluded from the above discussions that the confinement effect of the hard sphere on the fine-structure energy levels of the He-like Ar ion increases with decreasing the hard sphere radius.

3.3. Fine-structure energy levels in dense plasmas

The energy eigenvalues of 1s^2, 1s2s, and 1s2p atomic states for the He-like Ar ion in dense plasmas are displayed in Table 3. By comparing the data in Tables 2 and 3, it can be concluded that the energy eigenvalues are upshifted by free electrons, compared with the hard sphere confinement, very significantly. The energy levels of 1s2s and 1s2p atomic states for the He-like Ar ion in dense plasmas are listed in Table 4 and displayed in Fig. 5. It is shown from Fig. 5 that all energy levels decrease with increasing free electron densities. The reasons for this result are expressed below. The energy eigenvalue shift is the difference between energy eigenvalue of the ion immersed in plasmas and that in free case. As shown from Fig. 6, although energy eigenvalue shifts of all atomic states increase with increasing free electron densities, the extents of energy eigenvalue shifts for 1s^2 atomic state are always greater than those of the other atomic states. Thus the energy levels of all atomic states decrease with the rise of free electron density.

Table 3. The energy eigenvalues E (in a.u.) of $1s^2$, 1s2s, and 1s2p atomic states for the He-like Ar ion in dense plasmas.

R_0/a.u.	n_f/cm^{-3}	$1s^2$ ($^1S_0$)	1s2s ($^3S_1$)	1s2s ($^1S_0$)	1s2p ($^3P_0$)	1s2p ($^3P_1$)	1s2p ($^3P_2$)	1s2p ($^1P_1$)
5.0	2.06(23)	–304.5530343	–190.4704439	–189.7143767	–189.7984727	–189.7568906	–189.6497872	–189.1463013
3.0	9.55(23)	–298.1574386	–184.1042909	–183.3493778	–183.4238895	–183.3823705	–183.2754355	–182.7726644
2.0	3.22(24)	–290.1707806	–176.2071779	–175.4557956	–175.5011596	–175.4598333	–175.3534121	–174.8528217
1.5	7.64(24)	–282.1967607	–168.4091097	–167.6647614	–167.6528507	–167.6119064	–167.5065034	–167.0102471
1.4	9.39(24)	–279.9213798	–166.2043072	–165.4628171	–165.4279316	–165.3871417	–165.2821496	–164.7876612
1.3	1.17(25)	–277.2977768	–163.6752139	–162.9375825	–162.8719446	–162.8313620	–162.7269211	–162.2348076
1.2	1.49(25)	–274.2395873	–160.7466353	–160.0143453	–159.9065759	–159.8662770	–159.7625889	–159.2737673
1.1	1.94(25)	–270.6294004	–157.3192798	–156.5945923	–156.4275530	–156.3876479	–156.2849992	–155.8008598
1.0	2.58(25)	–266.3034846	–153.2601802	–152.546604	–152.2936398	–152.2542793	–152.1530443	–151.6758531
0.9	3.54(25)	–261.0265665	–148.3896503	–147.6925583	–147.3107605	–147.2721080	–147.1726257	–146.7062062
0.8	5.03(25)	–254.4482579	–142.4671065	–141.7943025	–141.2117251	–141.1737828	–141.0757348	–140.6266542
0.7	7.52(25)	–246.0235102	–135.1937869	–134.5547768	–133.6470619	–133.6091060	–133.5094632	–133.0896592

Table 4. The energy levels E_l (in cm^{-1}) of 1s2s and 1s2p atomic states for the He-like Ar ion in dense plasmas.

R_0/a.u.	n_f/cm^{-3}	1s2s ($^3S_1$)	1s2s ($^1S_0$)	1s2p ($^3P_0$)	1s2p ($^3P_1$)	1s2p ($^3P_2$)	1s2p ($^1P_1$)
5.0	2.06(23)	25038234	25204172	25185715	25194841	25218348	25328850
3.0	9.55(23)	25031773	25197457	25181103	25190216	25213685	25324031
2.0	3.22(24)	25012120	25177029	25167073	25176143	25199500	25309367
1.5	7.64(24)	24973503	25136868	25139482	25148469	25171602	25280518
1.4	9.39(24)	24958013	25120751	25128407	25137360	25160403	25268930
1.3	1.17(25)	24937270	25099161	25113567	25122474	25145396	25253403
1.2	1.49(25)	24908824	25069543	25093196	25102040	25124797	25232081
1.1	1.94(25)	24868697	25027747	25064408	25073167	25095695	25201952
1.0	2.58(25)	24810138	24966749	25022269	25030907	25053126	25157857
0.9	3.54(25)	24720946	24873940	24957735	24966218	24988052	25090419
0.8	5.03(25)	24577022	24724685	24852546	24860874	24882393	24980955
0.7	7.52(25)	24324313	24464559	24663780	24672110	24693979	24786115

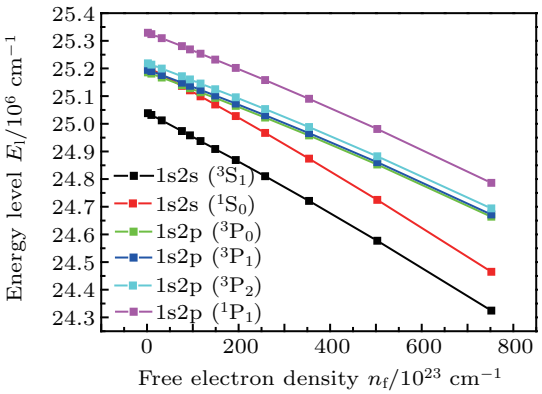


Fig. 5. (color online) The energy levels of 1s2s and 1s2p atomic states for the He-like Ar ion in dense plasmas.

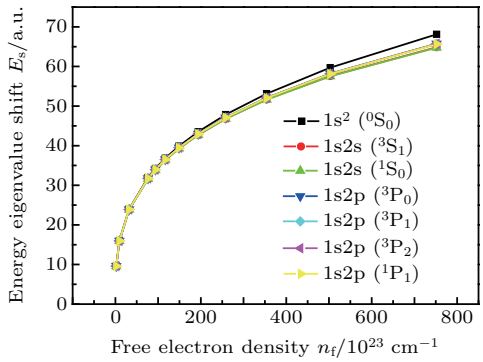


Fig. 6. (color online) The energy eigenvalue shifts of 1s2s and 1s2p atomic states for the He-like Ar ion in dense plasmas.

An interesting phenomenon about "energy level crossing" is found from Fig. 5. The energy level of 1s2s ($^1S_0$) state lies above that of 1s2p ($^3P_{0,1}$) states for free electron density $n_f \leq 3.22 \times 10^{24}$ cm^{-3} ($R_0 \geq 2.0$ a.u.), including the free case for $n_f = 0$ ($R_0 = \infty$). However, the energy level of 1s2s ($^1S_0$) state lies below that of 1s2p ($^3P_{0,1}$) after free electron density $n_f \geq 7.64 \times 10^{24}$ cm^{-3} ($R_0 \leq 1.5$ a.u.). This interesting phenomenon can be interpreted using Fig. 7. It is shown in Fig. 7 that the amount of energy level shift (decrease) of 1s2s ($^1S_0$) state is greater than those of 1s2p ($^3P_{0,1}$) states after free electron density $n_f \geq 7.64 \times 10^{24}$ cm^{-3} ($R_0 \leq 1.5$ a.u.), thus leading to that 1s2s ($^1S_0$) level lies blow 1s2p ($^3P_{0,1}$) levels. The "energy level crossing" phenomenon shows that an incidental degeneracy[29] has taken place among the 1s2s ($^1S_0$) and 1s2p ($^3P_{0,1}$) atomic states of the Ar^{16+} ion at some free electron density 3.22×10^{24} cm^{-3} $< n_f <$ 7.64×10^{24} cm^{-3} (1.5 a.u.$< R_0 <$ 2.0 a.u.), and then a level crossing occurs among these three atomic states having different symmetry properties. By the way, such incidental degeneracy and subsequent level crossing phenomenon have been found in case of cage confined H^- ion[30] and He atom,[31] He^+ ion in quantum dot,[32] and He-like ions within strongly coupled plasma environment.[12,13,15,18]

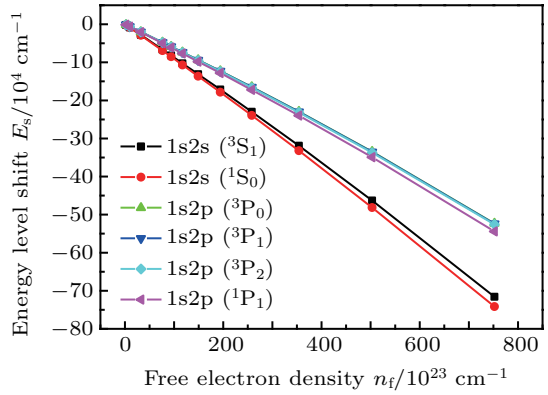


Fig. 7. (color online) The energy level shifts of 1s2s and 1s2p atomic states for the He-like Ar ion in dense plasmas.

As shown in Fig. 5, the energy level gap between states having the same symmetry decreases, but that between states having different symmetry increases, with increasing free electron densities. That is, the energy level gaps between states 1s2s (^{3}S$_1$) and 1s2s (^{1}S$_0$), 1s2p (^{3}P$_{0,1,2}$) and 1s2p (^{1}P$_1$) decrease respectively, but that between states 1s2s(^{1}S$_0$) and 1s2p (^{3}P$_0$) increases, with increasing free electron densities.

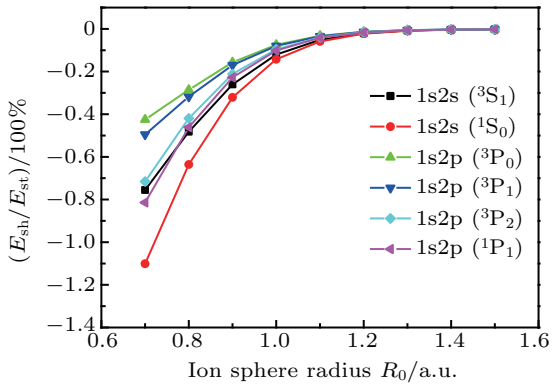


Fig. 8. (color online) The energy level shifts caused by the hard sphere confinement as a percentage of total energy level shifts of 1s2s and 1s2p atomic states for the He-like Ar ion in dense plasmas. E_{sh} is the energy level shift caused by the hard sphere confinement and E_{st} is the total energy level shift caused by the hard sphere confinement and free electron screening.

It is also shown in Figs. 7 and 2 that the direction of energy level shift caused by free electron screening is different from that caused by hard sphere confinement, namely, free electrons decrease energy levels but hard sphere confinement lifts energy levels. Therefore, the impact of the hard sphere confinement on the energy levels in dense plasmas is discussed here. It can be seen from Fig. 8 that the energy level shifts caused by the hard sphere confinement as a percentage of total energy level shifts of 1s2s and 1s2p atomic states for the He-like Ar ion in dense plasmas increase with decreasing the ion sphere radius (increasing the free electron density), and the highest percentage is -1.10% for 1s2s (^{1}S$_0$) state at $R_0 = 0.7$ a.u. (free electron density $n_f = 7.52 \times 10^{25}$ cm^{-3}). Thus we can conclude that the contribution of the hard sphere confinement to the fine-structure energy levels of the He-like Ar ion in dense plasmas, compared with that of free electron screening, is relative small and can be neglected generally.

However, there will not exist hard confinement but some kind of penetrable confinement, if the boundary condition that the radial wavefunctions gradually decay to zero outside of the ion sphere is used. This boundary condition has been used by Belkhiri *et al.*[13,33] and Li *et al.*[34] Of course, the most widely used boundary condition is that the radial wavefunctions are directly set as zero outside of the ion sphere (present case).[18,19,35–41] In addition, the two boundary conditions both have shortcomings. The boundary condition that the radial wavefunctions always equal to zero outside of the ion sphere is corresponding to that the electrostatic potential is equal to ∞ outside of the ion sphere, but the real potential is equal to zero outside of the ion sphere. The boundary condition that the radial wavefunctions gradually decay to zero outside of the ion sphere could not well maintain electrical neutrality of the whole ion sphere, because the bound electrons can move to outside of the ion sphere.

4. Conclusion

In this work, the fine-structure energy levels of 1s2s and 1s2p atomic states of the He-like Ar ion are calculated in the hard sphere confinement (no free electrons) and in dense plasmas (hard sphere confinement together with free electrons), respectively. The results show that under the only hard sphere confinement, all energy eigenvalues are shifted to continuum states, all energy levels are upward moved, the energy level separation shift is different between different energy levels, and the confinement effect of the hard sphere increases with decreasing the hard sphere radius. In dense plasmas, all energy levels decrease with increasing free electron densities; an "energy level crossing" phenomenon takes place among 1s2s (^{1}S$_0$) and 1s2p (^{3}P$_{0,1}$) atomic states while they are effectively bound states; the energy level gap between states having the same symmetry decreases, but that between states having different symmetry increases, with increasing free electron densities. The confined effect of the hard sphere on the fine-structure energy levels, compared with the contribution from free electron screening, can be neglected generally.

Acknowledgment

The authors express sincere gratitude to Prof. Jönsson P for free providing the GRASP2K program.

References

[1] Son S K, Thiele R, Jurek Z, Ziaja B and Santra R 2014 *Phys. Rev. X* **4** 031004
[2] Moses E I, Boyd R N, Remington B A, Keane C J and Al-Ayat R 2009 *Phys. Plasmas* **16** 041006

[3] Emma P, Akre R, Arthur J, Bionta R, Bostedt C, Bozek J, Brachmann A, Bucksbaum P, Coffee R, Decker F J, Ding Y, Dowell D, Edstrom S, Fisher A, Frisch J, Gilevich S, Hastings J, Hays G, Hering P, Huang Z, Iverson R, Loos H, Messerschmidt M, Miahnahri A, Moeller S, Nuhn H D, Pile G, Ratner D, Rzepiela J, Schultz D, Smith T, Stefan P, Tompkins H, Turner J, Welch J, White W, Wu J, Yocky G and Galayda J 2010 *Nat. Photonics* **4** 641

[4] Ishikawa K L and Ueda K 2012 *Phys. Rev. Lett.* **108** 033003

[5] Hoarty D J, Allan P, James S F, Brown C R D, Hobbs L M R, Hill M P, Harris J W O, Morton J, Brookes M G, Shepherd R, Dunn J, Chen H, Marley V E, Beiersdorfer P, Chung H K, Lee R W, Brown G and Emig J 2013 *Phys. Rev. Lett.* **110** 265003

[6] Ciricosta O, Vinko S M, Chunget H K, Cho B I, Brown C R D, Burian T, Chalupsky J, Engelhorn K, Falcone R W, Graves C, Hajkova V, Higginbotham A, Juha L, Krzywinski J, Lee H J, Messerschmidt M, Murphy C D, Ping Y, Rackstraw D S, Scherz A, Schlotter W, Toleikis S, Turner J J, Vysin L, Wang T, Wu B, Zastrau U, Zhu D, Lee R W, Heimann P, Nagler B and Wark J S 2012 *Phys. Rev. Lett.* **109** 065002

[7] Ciricosta O, Vinko S M, Barbrel B, Rackstraw D S, Preston T R, Burian T, Chalupský J, Cho B I, Chung H K, Dakovski G L, Engelhorn K, Hájková V, Heimann P, Holmes M, Juha L, Krzywinski J, Lee R W, Toleikis S, Turner J J, Zastrau U and Wark J S 2016 *Nat. Commun.* **7** 11713

[8] Fletcher L B, Kritcher A L, Pak A, Ma T, Döppner T, Fortmann C, Divol L, Jones O S, Landen O L, Scott H A, Vorberger J, Chapman D A, Gericke D O, Mattern B A, Seidler G T, Gregori G, Falcone R W and Glenzer S H 2014 *Phys. Rev. Lett.* **112** 145004

[9] Kraus D, Chapman D A, Kritcher A L, Baggott R A, Bachmann B, Collins G W, Glenzer S H, Hawreliak J A, Kalantar D H, Landen O L, Ma T, Pape S L, Nilsen J, Swift D C, Neumayer P, Falcone R W, Gericke D O and Döppner T 2016 *Phys. Rev. E* **94** 011202(R)

[10] Ecker G and Kröll W 1963 *Phys. Fluids* **6** 62

[11] Stewart J C and Jr Pyatt K D 1966 *Astrophys. J.* **144** 1203

[12] Li X D and Rosmej F B 2012 *J. Quant. Spectrosc. Ra.* **113** 680

[13] Belkhiri M and Poirier M 2013 *High Energy Dens. Phys.* **9** 609

[14] Ichimaru S 1982 *Rev. Mod. Phys.* **54** 1017

[15] Li X D and Rosmej F B 2010 *Phys. Rev. A* **82** 022503

[16] Rozsnyai B F 1991 *Phys. Rev. A* **43** 3035

[17] De M and Ray D 2015 *Phys. Plasmas* **22** 054503

[18] Bhattacharyya S, Saha J K and Mukherjee T K 2015 *Phys. Rev. A* **91** 042515

[19] Sil A N, Anton J, Fritzsche S, Mukherjee P K and Fricke B 2009 *Eur. Phys. J. D* **55** 645

[20] Woolsey N C, Hammel B A, Keane C J, Back C A, Moreno J C, Nash J K, Calisti A, Mosse C, Stamm R, Talin B, Asfaw A, Klein L S and Lee R W 1998 *Phys. Rev. E* **57** 4650

[21] Das M, Chaudhuri R K, Chattopadhyay S, Mahapatra U S and Mukherjee P 2011 *J. Phys. B-At. Mol. Opt.* **44** 165701

[22] Grant I P 1994 *Comput. Phys. Commun.* **84** 59

[23] Jönsson P, Gaigalas G, Bieroń J, Fischer C F and Grant I P 2013 *Comput. Phys. Commun.* **184** 2197

[24] Jönsson P, He X, Fischer C F and Grant I P 2007 *Comput. Phys. Commun.* **177** 597

[25] NIST Database or the paper written by Saloman E B 2010 *J. Phys. Chem. Ref. Data* **39** 033101

[26] Montgomery H E and Pupyshev V I 2015 *Theor. Chem. Acc.* **134** 1598

[27] Bhattacharyya S, Saha J K, Mukherjee P K and Mukherjee T K 2013 *Phys. Scr.* **87** 065305

[28] Yakar Y, Akir B and Özmen A 2011 *Int. J. Quantum Chem.* **111** 4139

[29] Sen K D 2005 *J. Chem. Phys.* **122** 194324

[30] Chandra R, Dutta B, Saha JK, Bhattacharyya S and Mukherjee T K 2018 *Int. J. Quantum Chem.* e25597

[31] Saha J K, Bhattacharyya S and Mukherjee T K 2016 *Int. J. Quantum Chem.* **116** 1802

[32] Saha J K, Bhattacharyya S and Mukherjee T K 2016 *Commun. Theor. Phys.* **65** 347

[33] Belkhiri M and Fontes C J 2016 *J. Phys. B-At. Mol. Opt.* **49** 175002

[34] Li X F, Jiang G, Wang H B and Sun Q 2017 *Phys. Scr.* **92** 075401

[35] Das M, Sahoo B K and Pal S 2016 *Phy. Rev. A* **93** 052513

[36] Salzmann D and Szichman H 1987 *Phys. Rev. A* **35** 807

[37] Saha B and Fritzsche S 2007 *J. Phys. B-At. Mol. Opt.* **40** 259

[38] Li Y Q, Wu J H, Hou Y and Yuan J M 2009 *J. Phys. B-At. Mol. Opt.* **42** 235701

[39] Li X D, Xu Z and Rosmej F B 2006 *J. Phys. B-At. Mol. Opt.* **39** 3373

[40] Li Y Q, Wu J H, Hou Y and Yuan J M 2008 *J. Phys. B-At. Mol. Opt.* **41** 145002

[41] Li X F, Jiang G, Wang H B and Sun Q 2017 *Chin. Phys. B* **26** 013101